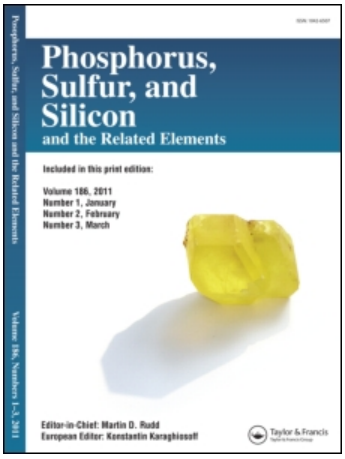

Phosphorus, Sulfur, and Silicon and the Related Elements
Publication details, including instructions for authors and subscription information:
http://www.informaworld.com/smpp/title~content=t713618290

STRUCTURAL DISTORTIONS OF CYCLIC PHOSPHORANES AND THE BERRY EXCHANGE COORDINATE. A QUANTITATIVE DESCRIPTION

Robert R. Holmes[a]; Joan A. Deiters[a]
[a] Contribution from the Department of Chemistry, University of Massachusetts, Amherst, Massachusetts

To cite this Article Holmes, Robert R. and Deiters, Joan A.(1995) 'STRUCTURAL DISTORTIONS OF CYCLIC PHOSPHORANES AND THE BERRY EXCHANGE COORDINATE. A QUANTITATIVE DESCRIPTION', Phosphorus, Sulfur, and Silicon and the Related Elements, 98: 1, 105 — 124
To link to this Article: DOI: 10.1080/10426509508036945
URL: http://dx.doi.org/10.1080/10426509508036945

Phosphorus, Sulfur, and Silicon, 1995, Vol. 98, pp. 105–124
Reprints available directly from the publisher
Photocopying permitted by license only

STRUCTURAL DISTORTIONS OF CYCLIC PHOSPHORANES AND THE BERRY EXCHANGE COORDINATE. A QUANTITATIVE DESCRIPTION†

ROBERT R. HOLMES* and JOAN A. DEITERS

Contribution from the Department of Chemistry, University of Massachusetts, Amherst, Massachusetts 01003

(Received September 17, 1976)

Structural distortions of cyclic phosphoranes are shown to form a continuous series between the idealized trigonal bipyramidal (D_{3h}) and square pyramidal (C_{4v}) representations. The particular form of the distortions is along the Berry intramolecular exchange coordinate. Despite the lack of symmetry in the makeup of the cyclic substituents, a local C_{2v} constraint is closely followed. The origin of the mode of distortion is discussed in relation to the two sets of bond properties peculiar to five-coordinate geometries and the closeness in energy of the two idealized structures, enhanced by the presence of ring constraints. These findings reinforce the operation of successive Berry rearrangements postulated to account for NMR exchange data on a wide variety of phosphorane derivatives.

An intriguing problem in five-coordinate chemistry concerns the detailed reaction coordinate followed by nonrigid phosphoranes undergoing polytopal rearrangement. For many derivatives, successive ligand permutations are necessary to adequately account for NMR data obtained over wide temperature ranges.[2] The favored mechanism for ligand rearrangement is the Berry process.[3] For example, the apparent equivalence of the methylene hydrogen atoms of the ethoxy groups observed[4] in the ^{1}H NMR spectrum of I, obtained at 100°C, is accountable by a minimum of five pseudorotations via the Berry mechanism in which each group bonded to phosphorus is used as a pivotal group.

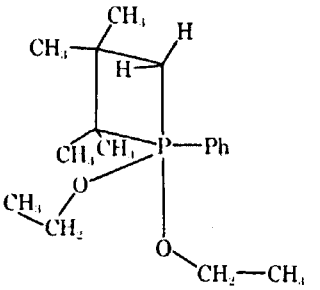

I

In any particular Berry pseudorotation, intramolecular deformation is achieved by a concerted bending of axial and equatorial ligand pairs. A C_{2v} symmetry constraint is implied when all ligands are alike. The exchanging D_{3h} ground state

†Reprinted with permission from *J. Am. Chem. Soc.*, **99**, 3318 (1977). Copyright 1977 American Chemical Society.

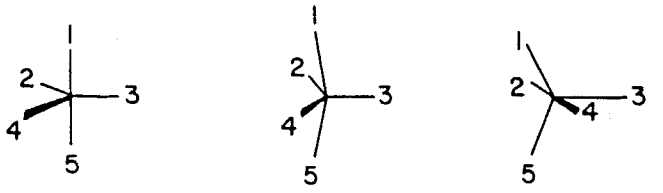

FIGURE 1 Berry exchange mechanism for the case involving all like ligands with position 3 as the pivotal ligand.

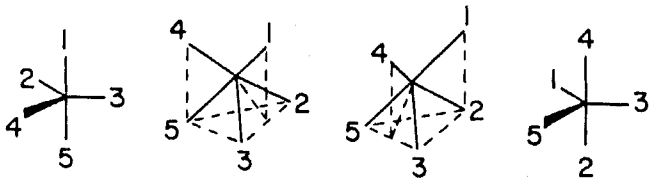

FIGURE 2 Turnstile exchange for MX_5 showing permutational equivalence with the Berry process (Figure 1). An equatorial in-plane bend decreases the angle 3–6–2 toward 90°, accompanied by a simultaneous rotation of atoms 4 and 1 relative to the other three atoms. Superimposed on these motions, atoms 4 and 1 also tilt to place them in equivalent positions relative to the triangular base atoms. The barrier structure is halfway between the two center structures shown here and is called a 30° TR.[5]

structure passes through a square pyramidal intermediate (C_{4v}) on the way to the "pseudorotated" conformer (Figure 1).

For the example cited above (I), symmetry is lacking in the ground state representation and should bear some degree of structural deviation from the idealized trigonal bipyramid. As a consequence, there is no a priori reason to expect that the Berry exchange pathway ($D_{3h} = C_{4v} = D_{3h}$) should be closely followed. In fact, a permutationally equivalent exchange mechanism has been advanced,[5] the turnstile process (Figure 2), which is governed by different symmetry conditions.

In theory, it should be possible to differentiate between mechanistic alternatives since different reaction coordinates are involved in each. In practice this has not been achieved. A possible approach is suggested by the recent characterization of cyclic phosphorane structures II by x-ray diffraction[6] which more closely approximate an idealized square pyramid[7] (the intermediate structural type in the Berry process), rather than the idealized trigonal bipyramid. By quantitative examination of structural distortions of a suitable series of phosphorane structures that extends incrementally from one idealized form to the other, and measurement of the magnitude that each individual structure deviates from a defined reaction coordinate, it may be possible to establish whether a preference for a particular pathway exists. In the subsequent presentation, two methods will be employed, one based on the

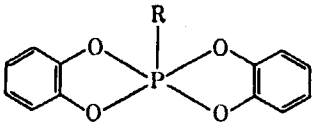

R = CH_3, F

II

measured angles at phosphorus and the other, first applied to five-coordinate complexes by Muetterties and Guggenberger,[8] based on dihedral angles.

The purpose of the present paper is to show that application of the latter technique does indeed allow differentiation among exchange coordinates and leads to the Berry coordinate as the one governing structural deviations of cyclic phosphoranes. Succeeding papers[9–11] in this series refer to the structural elucidation of some key members that form the basis of the present interpretation.

QUANTITATIVE ASSESSMENT OF STRUCTURAL DISTORTIONS

Sum of Angles Method

Three basic structures are considered: the trigonal bipyramid (TP), the square pyramid (SP), and the turnstile representation (TR). Idealized geometries for these representations are shown in Figure 3. The square pyramid shown represents the barrier state in the Berry exchange mechanism[3] while the 30° turnstile geometry is the barrier structure in the proposed[5] turnstile exchange process.

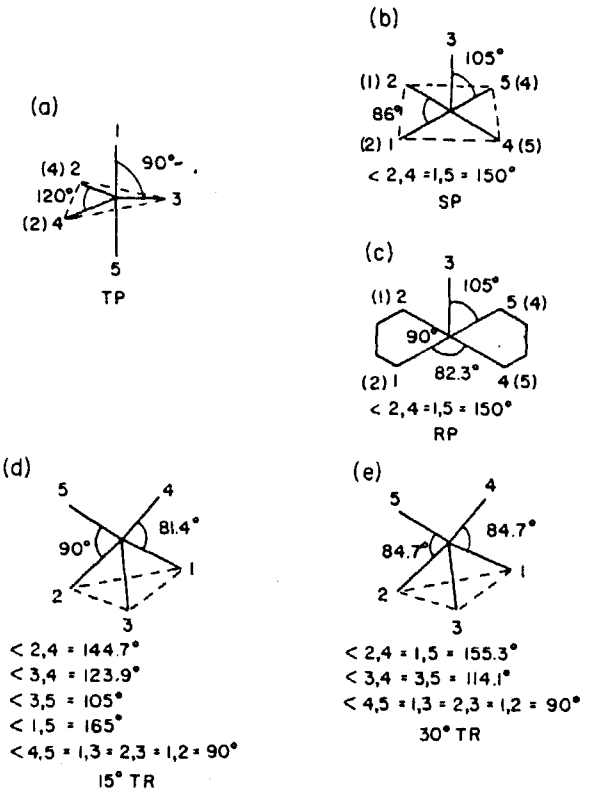

FIGURE 3 Idealized geometries: (a) trigonal bipyramid (TP); (b) square pyramid (SP); (c) rectangular pyramid (RP); (d) 15° turnstile (TR); (e) 30° turnstile (TR). The numbering scheme is not unique, although in representations (a)–(c) the only other possibility allowed is shown in parentheses which interchanges ligands only in the base planes.

In phosphoranes containing two five-membered rings, the observed internal ring angle at phosphorus is close to 90°. Hence, for these derivatives, a rectangular pyramid (RP) rather than a SP is a better representation of the barrier state in the Berry process. Angles for a 15° TR, representing a possible point along a turnstile exchange coordinate, are given in Figure 3 as well. The 15° TR geometry has been discussed as a preferred model for structural deviations of the catechol derivative III.[12]

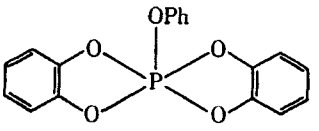

III

As discussed in other articles[9-11] in this series, we have determined the molecular structures of a number of cyclic phosphoranes by x-ray diffraction. Together with structural data on other cyclic derivatives which have appeared in the recent literature,[6,12-16] including the first crystal structure of an oxyphosphorane[15a] and x-ray parameters kindly supplied by Dr. W. S. Sheldrick[17-21] on his interesting series of bicyclic and spiro phosphoranes, sufficient information is at hand to critically examine the magnitude and direction of structural deviations from idealized representations given in Figure 3. The structures that will concern us are depicted in Figure 4 along with literature references. The caption for Figure 4 indicates the ligand numbering which determines the specific connecting idealized representations for each derivative as referenced in Figure 3.

The results on these cyclic pentacoordinate phosphorus compounds are summarized in Table I. For each compound designated in column 1, the sum of the observed angle deviations from each of the idealized structures, the TP, SP (or RP if two five-membered rings are present), the 15° TR, and the 30° TR configuration, is listed in columns 2, 3, 7, and 10, respectively. The sum represents the deviations of the ten angles involving the phosphorus atom in each of the structures.

It matters which ligand is taken as the single axial atom in the SP (RP), or which set of atoms forms the pair in the TR configuration, for purposes of calculating structural deviations. For all derivatives, various possibilities were examined, if not obvious, to define the ligands in such a way that the minimum sum of angular deviations from the idealized SP (RP) and TR representations is obtained. This was particularly important for ligand definitions relative to the idealized turnstile geometries shown in Figure 3.

Since the sum of the ten angular changes encountered on going from the TP to the SP geometry is 136° (135.4° for the RP), the values in column 3 are subtracted from 136° (or 135.4° for the RP representation) to obtain the values listed in column 4. In other words, if structural distortions follow a Berry coordinate, the values in columns 2 and 4, which are now both referenced as distortion sets with the idealized TP as 0°, should be the same. The extent to which they individually deviate is shown in column 6.[22] For comparisons among the various derivatives, an average value of structural distortion (average of columns 2 and 4) is given in column 5.

Considering the variety of ground state structures with their lack of symmetry, individual ring strain, and steric effects, it is remarkable that the structural distor-

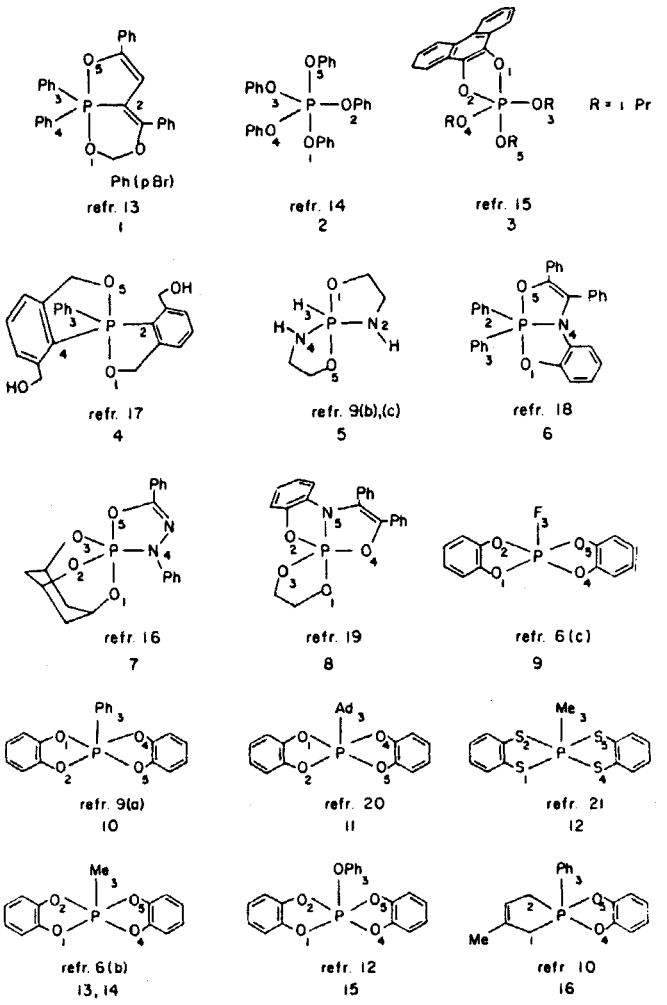

FIGURE 4 Compound number identification of structures referred to in Tables I, II, and III. In all of these structures ligands 2, 3, and 4 are oriented equatorial in a (TP) frame. In a SP or RP representation, ligand 3 is the axial ligand and ligands 2 and 4 have residual equatorial TP character. All the structures show distortions from idealized representations. They are given here in a form closest to one of the idealized representations. To redraw the structures in terms of other idealized representations, use this ligand numbering scheme relative to that shown in Figure 3. The best 30° TR structures are obtained from the ligand numbering and reference to Figure 3(e) except for entries **3** and **15**. See footnote *a* to Table I for these derivatives. For entry **11**, Ad = adamantyl. For entry **7**, the x-ray structure[16b] of the related compound with a $C(CF_3)_2$ group in place of the equatorial N–Ph group shows very similar bond parameters. The ligand numbering is the same as shown here for **7** except for the interchange of 2 and 3. The dihedral angle method (cf. Table III) shows the structure displaced 34% along the Berry coordinate toward the SP.

tions follow the Berry exchange coordinate so closely. This correspondence is shown in Figure 5 where the angular distortions summed from each of the two idealized geometries, the TP and SP (RP), are plotted against each other (column 4 vs. column 2).

TABLE I

Structural distortions of cyclic phosphoranes based on the sum of the angles at phosphorus, deg

1 Entry[a]	2 $\Sigma_i\lvert\theta_i(C) - \theta_i(TP)\rvert = A$[b]	3 $\Sigma_i\lvert\theta_i(C) - \theta_i(SP)\rvert = B$[c]	4 $S - B = A^*$[d]	5 Av A $(A + A^*)/2$	6 $\lvert A - A^*\rvert$[e]	7[f] $\Sigma_i\lvert\theta_i(C) - \theta_i(15°\ TR)\rvert = C$	8 $T' - Cg = A'$	9 $\lvert A - A'\rvert$[h]	10[f] $\Sigma_i\lvert\theta_i(C) - \theta_i(30°\ TR)\rvert = D$	11 $T'' - Dg = A''$	12 $\lvert A - A''\rvert$[i] $= A''$
1	23.7	130.1	5.9	14.8	17.8	104.9	−7.7	31.4	126.5	4.1	19.6
2	24.4	115.8	20.2	22.3	4.2	95.8	1.4	23.0	121.4	9.2	15.2
3	31.1	113.1	22.9	27.0	8.2	88.3	8.9	22.2	109.7[a]	20.9	10.2
4	37.7	110.1 (RP)	25.3	31.5	12.4	87.7	9.5	28.2	109.3	21.3	16.4
5	34.1	110.5 (RP)	24.9	29.5	9.2	87.1	10.1	24.0	108.7	21.9	12.2
6	44.4	91.6	44.4	44.4	0.0	75.0	22.2	22.2	106.6	24.0	25.0
7	65.4	96.6	39.4	52.4	26.0	82.4	14.8	50.6	101.5	29.1	36.3
8	49.0	87.0	49.0	49.0	0.0	86.2	11.0	38.0	100.2	30.4	14.0
9	88.5	44.7 (RP)	90.7	89.6	2.2	77.1	20.1	68.4	85.3	45.3	43.2
10	102.7	32.7 (RP)	103.3	103.0	0.6	60.7	36.5	66.2	61.7	68.9	33.8
11	108.0	28.6 (RP)	106.8	107.4	1.2	66.8	30.4	77.6	63.8	66.8	41.2
12	108.7	32.9 (RP)	102.5	105.6	6.2	65.3	31.9	76.8	68.9	61.7	47.0
14	117.2	20.6 (RP)	114.8	116.0	2.4	69.8	27.4	89.8	61.6	69.0	48.2
15	120.3	29.6 (RP)	105.8	113.1	14.5	74.7	22.5	97.8	61.9[a]	68.7	51.6
16	118.8	32.2 (RP)	103.2	111.0	15.6	64.6	32.6	86.2	70.0	60.6	58.2

[a] Refer to Figure 4 for the phosphorane formula corresponding to the entry number. The ligand positioning of each entry for comparison with the idealized TP and SP (RP) structures is identified in Figure 4. For comparison with the idealized 15° TR and 30° TR of Figure 3, the ligand numbering in Figure 4 gives the best representation except for those value entries in column 10 indicated by a superscript (*a*). For entries 3 and 15, the best 30° TR representation is obtained by numbering the triad 543 instead of 123 indicated in Figure 3 (e) and 21 for the ligand pair instead of 45. [b] The sum of the absolute values of the differences of the ten observed angles at phosphorus for a specific phosphorane and the respective angles at phosphorus in the idealized TP (Figure 3 (a)). [c] Calculated as in *b*, except referenced to the idealized SP or RP depicted in Figure 3 (b) and (c), respectively. When the RP is the reference structure, it is indicated in parentheses in this column. [d] The symbol *S* indicates the value of the sum as defined in *b* when this sum is taken between the idealized TP and either the SP or RP (depicted in Figure 3 (a)–(c)). When the SP is used, $S = 136°$, when the RP is used, $S = 135.4°$. Thus, columns 2 and 4 are referenced from the TP end of the scale (with the TP end being 0°). If a Berry coordinate is strictly followed for structural distortions, columns 2 and 4 should have the same value for a specific entry. [e] The difference in absolute value between columns 2 and 4. A measure of the structural deviation from the Berry coordinate. [f] The data in columns 7–9 and 10–12 are calculated similarly to that discussed for columns 3, 4, and 6 in footnotes *c*, *d*, and *e*. Columns 7–9 refer to the 15° TR shown in Figure 3 (d) while columns 10–12 refer to the 30° TR (Figure 3 (e)). [g] The angle sum as defined in *b* when the sum is taken between the idealized TP and either the 15° TR (T′) or 30° TR (T″). For the 15° TR, $T' = 97.2°$; for the 30° TR, $T'' = 130.6°$. [h] The difference in absolute value between columns 2 and 8 as a measurement of the extent to which structures distort from an idealized TP to a 15° TR. [i] The difference in absolute value between columns 2 and 11 as a measure of the extent to which structures distort from an idealized TP to a 30° TR.

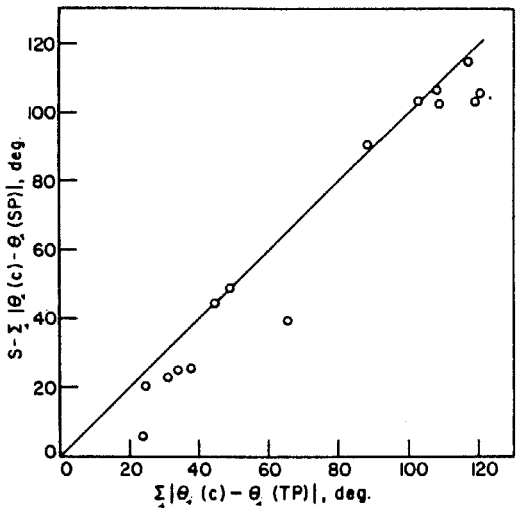

FIGURE 5 Cyclic phosphoranes showing distortion along the Berry exchange coordinate (solid line). The ordinate represents the sum of angular distortions of each compound from an idealized SP (RP) referenced to the same scale as used for the abscissa, $S - \Sigma_i|\theta_i(C) - \theta_i(SP)|$. The abscissa represents the sum of angular distortions for each compound from an idealized TP, $\Sigma_i|\theta_i(C) - \theta_i(TP)|$.

In contrast, a similar comparison for the turnstile pathway, that was illustrated in Figure 2, shows little correspondence between the angular deviations summed from the TP and TR geometries (cf. columns 2 and 8 of Table I for the 15° TR and columns 2 and 11 for the 30° TR). The reference value, the idealized TP structure taken as 0°, is the same for these comparisons as was used for the Berry pathway. In the calculation of the values in columns 8 and 11, the angular distortions summed from the 15 and 30° TR geometries (Figure 3) are subtracted from 97.2 and 130.6°, respectively. The latter values are the total angular changes over the ten phosphorus angles that take place on converting the idealized TP to the respective 15 and 30° TR configurations.

The data in columns 9 and 12 are instructive in that they show that as the observed structures distort away from the TP geometry toward the SP (RP) under the C_{2v} constraint of the Berry coordinate, the deviations from either turnstile geometry, in general, progressively increase. Furthermore, although the 15° TR, in general, gives a lower sum for the angular deviations about phosphorus compared to that for the 30° TR geometry (cf. columns 7 and 10), the 30° TR shows lower deviations referenced to a TP scale than does the 15° TR geometry (cf. columns 12 and 9).

Dihedral Angle Method

Perhaps a better method representing structural distortions is to calculate dihedral angles between triangular faces as outlined by Muetterties and Guggenberger[8] and examine these relative to the idealized TP and SP (RP) structures. If the calculation is performed using all observed angles and distances rather than only unit distances,[8] it is possible to evaluate the full effect of structural distortions. For example, as the structural distortion toward a SP occurs, the bond lengths as well

as the bond angles show evidence of residual TP character. The longer pair of bond lengths when like ligands are involved is associated with the larger trans basal angle of a SP (RP), indicative of the axial character of the TP, while the shorter pair of bond lengths is associated with the smaller trans basal angle, indicative of residual equatorial TP character (see references indicated in Figure 4 for structural parameters of compound entries **2**, **3**, **7–15**).

In a manner analogous to that of Muetterties and Guggenberger,[8] a plot of each trans basal angle, or what would be a trans basal angle if a SP were formed (angles 24 and 15 with reference to the ligand definitions given in Figure 3), vs. the dihedral angle δ_{24} undergoing the greatest change on going from the TP to the SP (RP) geometry, i.e., from 53.1° to 0°, is shown in Figure 6. The latter angle δ_{24} is that formed between normals to the TP faces, 124 and 245, which faces have the common equatorial edge 24 (Figure 3 (a)). This edge disappears in a SP or RP having four equal basal bond distances; thus, the dihedral angle becomes 0°. The corresponding data used in constructing Figure 6 are summarized in Table II.

The set of dihedral angles for each cyclic phosphorane is listed in Table III.[23] If we compare each dihedral angle for a specific compound with the corresponding values for the idealized TP and SP (RP) geometries and take these differences, we may compare the sum of the differences for each set on a common scale as was done for the sum of the ten angular deviations around phosphorus as discussed for Table I. The results of the new comparison are included in Table III. The scale is provided by the sum of the respective dihedral angle changes between the TP and

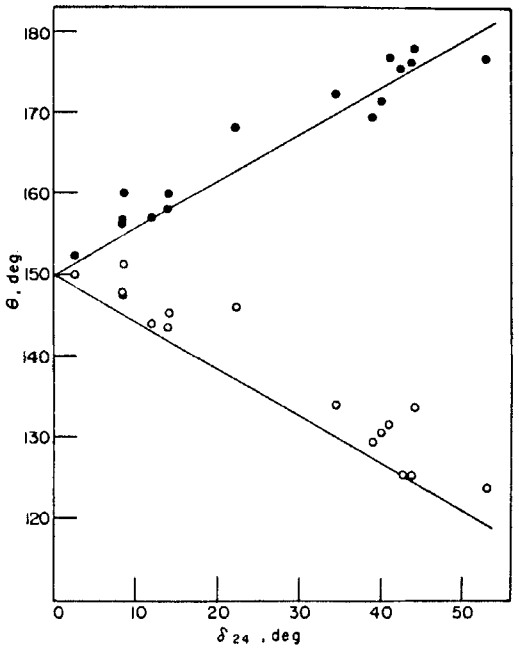

FIGURE 6 Variation of the angles at phosphorus θ_{15} (filled circles) and θ_{24} (open circles) vs. the dihedral angle δ_{24} as structural distortion proceeds along the Berry coordinate (solid lines) from a SP (RP) toward a TP.

TABLE II

Variation of the dihedral angle δ_{24} with the angles θ_{15} and θ_{24} at phosphorus, deg[a]

Entry[b]	δ_{24}	θ_{15}	θ_{24}
1	53.1	176.9	124.0
4	44.2	178.1	133.9
2	43.9	176.6	125.5
3	42.6	175.2	125.5
5	41.0	177.0	131.7
6	39.9	171.6	130.6
7	38.9	169.8	129.5
8	34.5	172.4	134.0
9	22.2	168.2	146.1
10	14.2	160.0	145.4
12	14.0	158.0	143.5
11	12.1	157.1	144.1
15	8.7	160.0	151.4
13	8.5	156.2	147.7
14	8.4	156.9	148.1
16	2.6	152.5	150.0

[a] With reference to Figure 3(a)-(c), the dihedral angle δ_{24} goes to zero as the Berry coordinate is traversed with ligand 3 as the pivotal ligand. The angles θ_{15} and θ_{24} at phosphorus then become trans basal angles in the SP (RP) representation. [b] Formula identification is given in Figure 4. Entries 13 and 14 are for the same compound which exhibits two slightly different structures in the unit cell. Structure I of ref 6b is labeled 14 here and structure II of ref 6b is entry 13.

SP (RP) geometries. This value is 217.9° for $\Sigma_i|\delta_i(\mathrm{TP}) - \delta_i(\mathrm{SP})|$ and 217.7° for $\Sigma_i|\delta_i(\mathrm{TP}) - \delta_i(\mathrm{RP})|$. For any compound C, the sums $\Sigma_i|\delta_i(\mathrm{C}) - \delta_i(\mathrm{TP})|$ and 217.9° $- \Sigma_i|\delta_i(\mathrm{C}) - \delta_i(\mathrm{SP})|$ should be the same if a Berry coordinate is followed for the structural distortions. The same expressions hold for the RP representation with the replacement of 217.9° by 217.7°. A plot of one sum vs. the other is shown in Figure 7.

The percent displacement along the Berry coordinate is given at the bottom of the column for each derivative in Table III. This value serves as a quantitative measure of the structural distortion. When viewed relative to the values of θ_{15} and θ_{24} for a specific substance (Table II), the principal features of the structural distortion are readily visualized.

If we calculate dihedral angle differences relative to the 30° TR idealized representation $\Sigma_i|\delta_i(\mathrm{C}) - \delta_i(30°\ \mathrm{TR})|$ from the data in Table III and subtract this difference for each compound from $T = 223.8°$ (the sum of dihedral angle changes between the idealized TP and 30° TR), a divergence between $T - \Sigma_i|\delta_i(\mathrm{C}) - \delta_i(30°\ \mathrm{TR})|$ and $\Sigma_i|\delta_i(\mathrm{C}) - \delta_i(\mathrm{TP})|$ is obtained which increases as we move further from the TP end of the scale (i.e., from derivative 1 to 16 in Table III). For the similarly structured derivatives 9–15, the average deviation between these two sums is ±16.0°; whereas, for the corresponding sums between the TP and RP, the average deviation is ±0.2°.

TABLE III

Dihedral angles (δ) for cyclic phosphoranes calculated from x-ray diffraction data, deg[a]

δ[b]	TP	1[c]	2	3	4		5	6	7	8	9	10	11	12	13	14	15	16	SP	RP	30° TR[d]	7[d] (for 30° TR)
45	101.5	102.6	107.6	107.0	104.7	106.6[e]	109.3	105.8	100.8	108.2	113.5	114.6	112.1	116.2	113.9	114.2	116.9	120.6	118.5	117.6	129.9	112.1
25	101.5	97.7	103.3	106.1	103.9	105.7	108.3	104.1	114.6	110.5	114.9	111.9	114.0	119.5	115.3	116.2	119.9	114.7	118.5	119.3	121.2	100.8
14	101.5	102.2	106.2	103.2	103.8	105.4	108.3	105.9	100.8	106.2	115.4	113.0	113.2	118.1	115.7	115.4	117.3	120.6	118.5	119.3	121.2	114.5
12	101.5	100.3	104.0	105.9	105.6	107.0	109.3	103.5	112.1	109.9	112.8	113.4	111.8	116.4	114.1	113.8	115.7	115.8	118.5	117.6	107.6	100.8
35	101.5	100.5	98.9	97.9	90.9	93.4	93.2	93.3	95.8	93.7	84.1	84.0	83.6	80.2	81.9	81.0	77.6	70.1	76.9	76.9	70.6	94.9
13	101.5	100.6	98.0	99.1	91.3	93.4	93.2	91.2	94.9	91.5	83.9	83.9	84.7	81.5	80.8	81.9	79.2	80.9	76.9	76.9	81.0	95.8
23	53.1	56.9	56.3	55.0	61.2	58.0	54.3	65.5	47.7	56.6	64.5	71.5	72.0	65.5	74.2	73.4	71.6	79.1	76.9	76.9	81.0	66.1
34	53.1	58.8	52.2	53.9	62.0	59.0	54.3	59.4	66.1	60.6	64.2	70.2	72.4	67.3	73.5	73.7	72.0	75.9	76.9	76.9	70.6	47.7
24	53.1	53.1	43.9	42.6	44.2	41.2	41.0	39.9	38.9	34.5	21.0	13.5	12.1	13.2	8.3	8.2	8.7	2.6	0.0	0.0	0.0	38.9
$\Sigma_i\lvert\delta_i(C) - \delta_i(TP)\rvert$		18.2	34.5	35.4	58.5	57.8	60.3	63.7	70.0	76.2	141.1	157.1	159.0	172.1	179.6	179.5	191.8	217.0				
$\Sigma_i\lvert\delta_i(C) - \delta_i(SP)\rvert$		206.7	185.2	182.5				154.2	161.5	141.7												
$S - \Sigma_i\lvert\delta_i(C) - \delta_i(SP)\rvert$[f]		11.2	32.7	35.4				63.7	56.4	76.2												
$\Sigma_i\lvert\delta_i(C) - \delta_i(RP)\rvert$					159.0	160.1	157.4				76.6	60.6	58.7	46.0	38.1	38.2	27.1	27.3				
$R - \Sigma_i\lvert\delta_i(C) - \delta_i(RP)\rvert$[g]					58.7	57.8	60.3				141.1	157.1	159.0	171.7	179.6	179.5	190.6	190.4				
ζ along Berry coor		2.2	15.4	16.3	26.9	26.5	27.7	29.2	29.0	35.0	64.8	72.1	73.0	78.9	82.4	82.4	87.7	93.3				

[a] The individual dihedral angles for the entries may be compared row for row, with those for the idealized representations TP, SP, RP, and 30° TR, except for that noted in *d*. [b] The individual dihedral angles δ are identifiable with reference to the numbering scheme in Figure 4 for the entries and Figure 3 for the idealized representations TP, SP, RP, and 30° TR. The ligand numbering in Figure 4 shows which group is deforming toward the axial position of the SP and which pair of ligand bonds have partial axial or partial equatorial character of the reference TP. The subscripts on δ refer to the common edge connecting the two triangular faces whose normals give the dihedral angle. [c] Refer to Figure 4 for the phosphorane corresponding to each of the numbered entries listed here in the top row. Entries 13 and 14 refer to two slightly different structures in the unit cell. Reference 6b identifies entry 13 as structure II and 14 as structure I. [d] For comparison of structural distortions from the 30° TR reference, all the dihedral angles for each entry are directly comparable, row for row, with the column labeled 30° TR. The numbering in Figure 4 for each entry compared to that in Figure 3e gives the closest 30° TR representation, except for entry 7. For the latter, a slightly closer representation results if the ligand numbers 2 and 3 are interchanged in Figure 4. [e] This column for structure 4 shows how the set of dihedral angles changes if the bond lengths are assumed to be all the same. [f] $S = \Sigma_i\lvert\delta_i(TP) - \delta_i(SP)\rvert = 217.7°$. This value represents the sum of dihedral angle changes on going from the idealized TP to the SP shown in Figure 3. [g] $R = \Sigma_i\lvert\delta_i(TP) - \delta_i(RP)\rvert = 217.9°$. This value represents the sum of dihedral changes on going from the idealized TP to the RP shown in Figure 3.

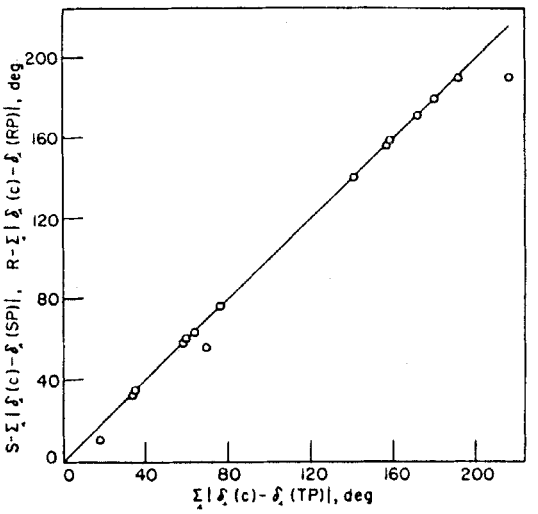

FIGURE 7 The sum of dihedral angles for cyclic phosphoranes from a SP (RP) idealized geometry vs. that from a TP geometry on a common reference scale. The solid line is along the Berry exchange coordinate. The point for structure **16** (farthest to the right) is off the line no doubt because of the presence of lattice disorder.[10]

DISCUSSION

The excellent degree to which distortions of cyclic phosphoranes under consideration here follow the local C_{2v} constraint of the Berry intramolecular exchange coordinate (Figures 5–7) is at first glance somewhat surprising. The nature of the ligand construction in many of the derivatives, the distortion expected because of the presence of ring constraints and steric effects of asymmetrically composed ligands, all argue for a variety of ground state structural forms unrelated to each other by a simple axial-equatorial bond bending motion. The fact that the latter motion is closely followed, in spite of the presence of the above factors, suggests that the origin of such distortions is inherent in the makeup of five-coordinate geometries.

Lattice effects which are expected to vary from one structure to another do not provide a consistent rationale for the distortions observed. In many of the structures, there are no close intermolecular contacts, which indicates the relative unimportance of this term in providing an underlying basis for the systematic trend in distortion between a TP and SP (RP) geometry.

If all bonds or positions could be equivalent in a five-coordinate structure, we might anticipate structural distortions to then be determined by the various factors mentioned above and provide an unrelated series of structures not tied by a common distortion mechanism. Because equivalent placement of five groups is geometrically impossible (except in a plane), two sets of ligand positions result. As theoretical[5a,24] and spectroscopic [25,26] evidence has shown, the TP and SP are structures close in energy. For example, in PF_5 the TP is estimated[25,26] to be more stable than the SP by about 4 kcal/mol. We have argued[1,7] that ring constraints in small-membered rings tend to favor a SP (RP) geometry. This point is amplified in following pa-

pers[9-11] in this series. Further, it is suggested that the series of compounds shown in Figure 4 provides a graded series defensible in terms of increasing constraints (ring, steric, etc.) enhancing the formation of a SP (RP).

According to theoretical treatments,[24a,b] the molecular orbitals for TP and SP easily transform into each other along the Berry coordinate ($D_{3h} \rightarrow C_{2v} \rightarrow C_{4v}$). The large vibrational amplitudes[27] and correspondingly low frequency[25,26,28] equatorial bending motions observed spectroscopically are manifestations of this effect and are directly related to the closeness in energy of the TP and SP conformations. Thus, the axial-equatorial bending motion associated with the Berry process will provide a low-energy coordinate which is readily traversed when higher energy constraints, as present with cyclic phosphoranes, are imposed. Steric and ring strains, for example, may cause energy differences for the TP and SP forms of cyclic derivatives exceeding the energy required, in their absence, to move completely from the TP to the SP. Depending on the particular ligand construction (bulky groups, ring effects, etc.), the point reached along the Berry coordinate (i.e., the minimum energy configuration) will be determined largely by which position proves most satisfactory in relieving these ligand repulsion and strain energies.

In another sense, the equatorial-axial bending motion may be viewed as having a very low force constant over wide angle variations. Hence, the presence of any perturbing influence, ring strain, steric strain, lattice effects, intermolecular hydrogen bonding, etc., will be relieved most readily by angular slippage to produce a minimum energy conformational balance. This balance will result as a compromise primarily between a tendency to reduce intramolecular energy terms (and to a lesser extent intermolecular energy terms) at the expense of moving toward the inherently higher energy associated with reaching the SP (RP) conformation. Thus, instead of seeking a structural minimum by deformations around a central atom involving more rigid bond angles (comparable in size), as appears to be the case with most compounds having coordination numbers 2, 3, 4, and 6, added flexibility is available in these cyclic phosphoranes by following a low energy bending coordinate to bring about a conformation which minimizes interactions and does so without appreciable deviation from the Berry coordinate. To do so would be more costly in energy.

We establish that this is the case by performing calculations based on conformational minimization techniques.[11] By allowing Berry coordinate to be traversed with little energy input, quantitative assessment results in a minimum energy conformation, for example, for derivative 13 (Figure 4), which agrees closely with the observed[6b] structure.

Structural Basis for Distortions

In general, movement along the Berry coordinate from the TP to the SP for the phosphoranes shown in Figure 4 (the SP becomes progressively more favored from structure **1** to **16**) appears to correlate with increasing cyclization (cf. **2, 3,** and **15**), especially with unsaturated rings,[1] and with decreasing electronegativity of the ligand regarding as the pivotal ligand which connects the idealized TP and SP for

each structure.[1,29] In addition, the preference of the more electronegative ligands for axial sites of a TP is apparent.[30]

In derivative **8,** an interesting situation arises. Owing to the cyclic construction, the less electronegative nitrogen atom is found at an apical position of the TP shown in Figure 4. This undesirable situation leads to considerable movement toward the SP. Although structure **16** has one ring with carbon atoms attached to phosphorus, movement away from the SP is inhibited by the resulting undesirable introduction of a ring carbon having residual axial character in a TP. Actually, the related derivative IV[31] having saturated rings, but a more highly strained four-membered ring, is estimated to be close to **13** in location along the Berry coordinate.

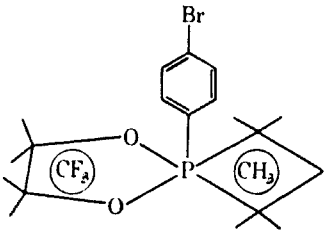

IV

Four-Membered Ring Systems

We have estimated the distortions in three four-membered ring phosphoranes,[31-33] V, VI, and VII, according to the dihedral angle method. These values are listed in Table IV and show distortions similar to derivatives **5** and **13** of Table III. Structures VI and VII are seen to be somewhat displaced from the Berry coordinate. The major portion of the deviations is no doubt associated with the strained angles at phosphorus in the four-membered ring systems.

TABLE IV

Dihedral angles (δ) for cyclic phosphoranes with four-membered rings, deg[a]

	Structure		
δ	V	VI	VII
1	107.0	112.6	111.5
2	102.3	102.3	116.8
3	110.1	109.0	114.0
4	110.6	100.1	123.9
5	96.0	93.4	81.3
6	90.6	99.4	80.7
7	69.3	76.4	69.9
8	52.7	40.3	75.5
9	40.8	38.1	5.8
$\Sigma_i\lvert\delta_i(C) - \delta_i(TP)\rvert$	61.1	82.1	187.7
$\Sigma_i\lvert\delta_i(C) - \delta_i(SP)\rvert$	159.4	164.2	41.0
$S - \Sigma_i\lvert\delta_i(C) - \delta_i(SP)\rvert$	58.5	53.7	176.7
% along Berry coor(av)	27.5	31.2	83.7

[a] See footnotes to Table III.

P—O Bond Distance Variations

All of the structures included in Figure 4 have one or more P—O bonds, except **12**. The most prevalent type of P—O bond in these derivatives is present in an unsaturated five-membered ring. Since the angle variations indicate structural distortions along a Berry coordinate, corresponding evidence should exist in bond distance variations. A graph of P—O bond distances vs. the dihedral angle function,

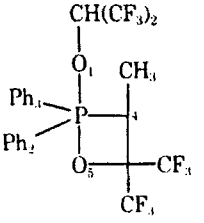

(ref. 33)

V

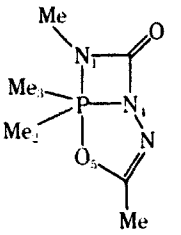

(ref. 32)

VI

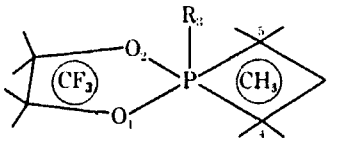

R = *p*-BrC$_6$H$_4$

(ref. 31)

VII

$\Sigma_i|\delta_i(C)-\delta_i(TP)|$ (cf. Table III), for each phosphorane is given in Figure 8. A list of pertinent P—O bond distances is summarized in Table V.

The variations displayed for P—O bond distances are entirely consistent with structural distortions along the TP-SP (RP) pathway. As the structural type comes closer to the idealized SP (RP), a convergence in P—O bond lengths occurs. Ring P—O bonds, which either have predominantly axial or equatorial character at the beginning of the series (Figure 4) and, consequently, a large disparity in bond distances, move to intermediate values as both types of bonds assume predominant basal character of the RP toward the end of the series. The range of values expected for P—O bonds in TP and SP (RP) geometries agrees with that calculated in an earlier study (refer to columns A and F of Table II in ref 1 and accompanying discussion).

There is an insufficient range of data to make similar plots for other types of P—O bonds. It should, however, be noted that axial P—O bond distances in saturated five-membered rings (as in derivative **5**) are about 0.05 Å less than in unsaturated rings and axial P—O bond distances in acyclic substituents, about 0.1 Å less (as in derivatives **2** and **3**) for compounds that are near TP in character. This indicates reduced strain in the five-membered saturated ring.[1] In accordance with this view, axial P—O bond distances in structures having four-membered rings, where ring strain should be enhanced, lie above the line in Figure 8 (cf. entries in Table IV). Hence, they are longer than those in comparable five-member rings.

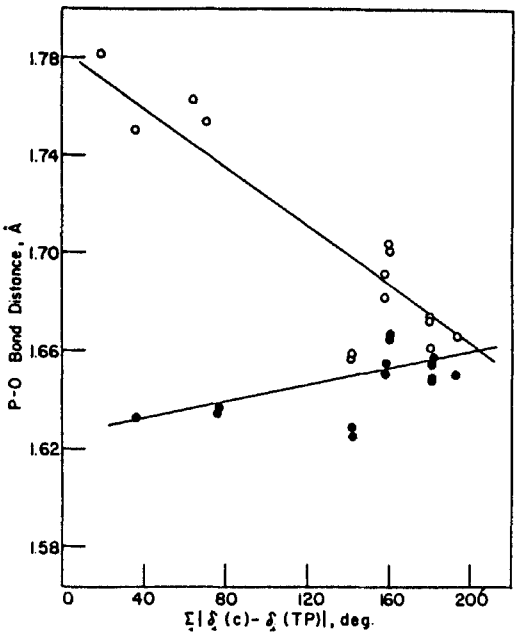

FIGURE 8 Variation of axial (upper line) and equatorial (lower line) P—O bond distances as structural distortion for five-membered unsaturated cyclic phosphoranes, measured by the dihedral angle sum $\Sigma_i|\delta_i(C) - \delta_i(TP)|$, proceeds along the TP – SP (RP) coordinate. The solid lines are least-squares lines excluding entry 9.

The relative strain effects in these rings in the TP and SP structures have been correlated[1,7] with variations in P—O π bonding and substituent electronegativity. Calculations[1] show that, owing to the equal character of basal bonds in a SP, ring strain is relaxed relative to the positioning of small-membered rings, especially unsaturated ones, in an axial-equatorial orientation of a TP having unequal bond character.

MECHANISTIC IMPLICATIONS

Intramolecular Exchange Phenomena

In accounting for temperature dependent NMR data indicating the onset of a variety of intramolecular ligand interchanges in a wide assortment of trigonal bipyramidal phosphorus compounds,[2] successive pseudorotations (Berry processes) have been invoked to reach proposed higher energy trigonal bipyramidal exchange intermediates. With the use of topological diagrams[34,35] the minimum number of coupled axial-equatorial bending motions required to reach the high energy intermediate may easily be determined, if not otherwise obvious. The close correspondence with the Berry coordinate for cyclic phosphoranes demonstrated here reinforces the operation of the Berry process for describing observed nonrigid behavior of phosphoranes. Accordingly, it appears likely that additional Berry processes occur, as

TABLE V

Phosphorus-oxygen bond distances in cyclic phosphoranes, Å

Entry[a]	$\Sigma\lvert\delta_i(C) - \delta_i(TP)\rvert$[b]	$P\text{-}O_{ax}$ (ring size[c])	$P\text{-}O_{eq}$ (ring size[c])
1	18.2	1.786($\bar{5}$)	
		1.737(6)	
2	34.5	1.662	1.602
		1.663	1.596
			1.600
3	35.4	1.751 ($\bar{5}$)	1.633 ($\bar{5}$)
		1.638	1.574
			1.588
4[d]	58.5	1.715 (5)	
		1.737 (5)	
5	60.3	1.709 (5)	
		1.709 (5)	
V	61.1	1.71	
		1.79 (4)	
6	63.7	1.700 ($\bar{5}$)	
		1.763 ($\bar{5}$)	
7	70.0	1.627 (6)	1.601 (6)
		1.754 ($\bar{5}$)	1.590 (6)
8	76.2	1.654 (5)	1.595 (5)
			1.635 ($\bar{5}$)
			1.637 ($\bar{5}$)
VI	82.1	1.798 ($\bar{5}$)	
9	141.1	1.659 ($\bar{5}$)	1.629 ($\bar{5}$)
		1.658 ($\bar{5}$)	1.625 ($\bar{5}$)
10	157.1	1.691 ($\bar{5}$)	1.650 ($\bar{5}$)
		1.682 ($\bar{5}$)	1.655 ($\bar{5}$)
11	159.0	1.701 ($\bar{5}$)	1.665 ($\bar{5}$)
		1.703 ($\bar{5}$)	1.667 ($\bar{5}$)
13	179.6	1.661 ($\bar{5}$)	1.658 ($\bar{5}$)
		1.674 ($\bar{5}$)	1.650 ($\bar{5}$)
14	179.5	1.672 ($\bar{5}$)	1.654 ($\bar{5}$)
		1.674 ($\bar{5}$)	1.649 ($\bar{5}$
VII	187.7	1.74 (5)	1.68 (5)
15	191.8	1.666 ($\bar{5}$)	1.666 ($\bar{5}$)
		1.666 ($\bar{5}$)	1.650 ($\bar{5}$)
			1.597

[a] Identified in Figure 4 or Table IV. [b] Structural distortion as measured by the sum of the dihedral angle differences relative to the idealized TP. These values are reported in Table III. [c] The symbols following the P-O bond distance values (references as reported in Figure 4 and under the structural formulas for V to VII) have the following meaning. The number in parentheses gives the ring size. A bar over the number indicates that the ring is unsaturated. If no number is given, the directly bonded ligand is acyclic. [d] The P-O bonds for entry 4 are not part of a similar ring system as other unsaturated five-membered rings considered here since the point of unsaturation is two bonds removed from the oxygen ligand. Hence, the P-O distances are most likely between values appropriate for a saturated and unsaturated five-membered ring.

postulated, to reach higher energy TP intermediates, but that these proposed intermediates may not be barrier states.

As an example, consider the isomerization route following a pseudorotational pathway for the adduct of dimethylphenylphosphonite and benzylideneacetylacetone.[35,36] For this process, which requires four successive Berry pseudorotations, we envision a potential energy description of the type where none of the levels are

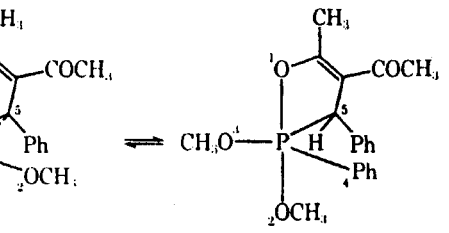

31 trans ⇌ **12** cis

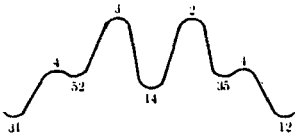

equal in energy. The number pairs in this topological representation (see ref 35) refer to axial positions of the TP and the single numbers refer to the apical ligand of the SP transition states. In related isomer pairs, 52 and 35, 4 and 4, 3 and 2, the phenyl group attached to the ring carbon atom is oriented differently relative to the other ligands. Consequently each member of the pair should differ slightly in energy from the other.

The initial ground state structure (31) should be near the TP end of the scale (perhaps near the structure of compound **4** of Figure 4). The first pseudorotation (31 → 52) must necessarily pass through a SP (4) having equal trans basal angles.

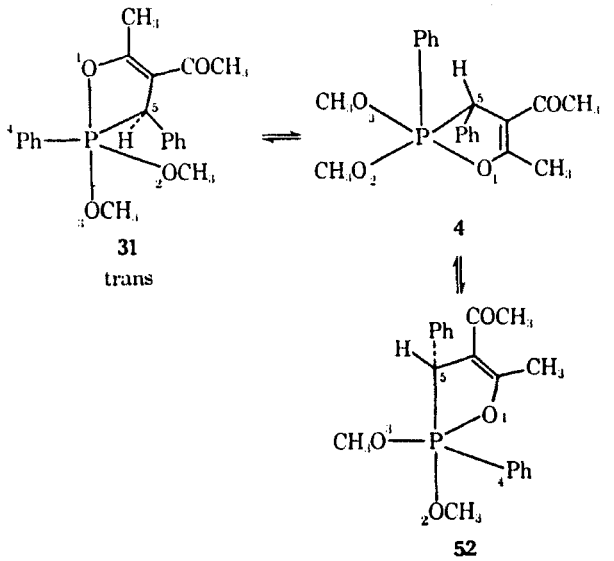

31 trans ⇌ **4** ⇌ **52**

We regard a point at or near this representation as having maximum ligand interaction and hence, a high energy formulation. The ligand exchanged intermediate (52) probably is considerably further along the TP-SP coordinate toward SP than 31 due to the unfavorable apical orientation of a carbon atom (operation of the electronegativity rule).[30b] Thus, the distortion produces a better balance of ligand interactions and the full apical character of the ring carbon is not realized. These factors should lead to a lower energy relative to the conformation discussed for **4**.

Each successive pseudorotation should be similar, the relative energy governed by the relative isomer energy gauged by substituent axiophilicities, ring constraints, and steric factors. Thus, 3 is shown higher than 4 because a less electronegative group is present in the axial position of the SP (4) relative to 3.[29] Isomer 14 should not be nearly as distorted from the TP compared to 52 because a more electronegative phenyl group has apical character instead of a ring carbon atom. Hence, isomer 14 should have a lower energy than 52. The isomerization process indicated by NMR data[35,36] is completed by two more pseudorotations completely analogous to the first two discussed above.

Structure **8** of Figure 4 is interesting in this regard. Were it not for the bicyclic nature of the tridentate ligand, the nitrogen atom would preferentially position itself equatorially in a near TP frame. As it is, the ring constraints tend to place the bridgehead nitrogen atom toward an apical position of the TP and the more electronegative ring oxygen equatorial. To counter this tendency, the ring system achieves better stability by becoming more planar as the structure distorts toward a SP. As a consequence, the ground state structure is found near the halfway point of the TP-SP coordinate (Figure 7). This gives us some idea of the distortion expected for isomer 52. The fact that the distortion of structure **8** is along the Berry pathway, in spite of its forced configuration, gives added credence to the operation of pseudorotations involving high-energy intermediates.

The adamantanoid derivative **7** and related substances show rapid positonal exchange[16] on the NMR time scale. As indicated in Figure 4, the structure of **7** is approximately 30% displaced (Table III) along the Berry coordinate toward the SP. This SP, which is a most likely representation of the transition state for ligand

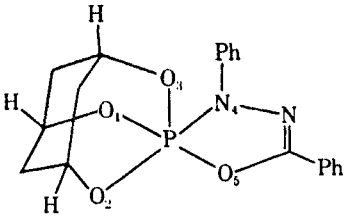

exchange in **7**, is easily reached by the axial-equatorial bending combination of the Berry process since the ground state TP is already considerably displaced toward this formation. Continuation of the bending action yields the intermediate TP, which, when followed by a second pseudorotation (P—O_1 is the pivotal bond) through a SP transition state similar to that above, completes the basic exchange mechanism.

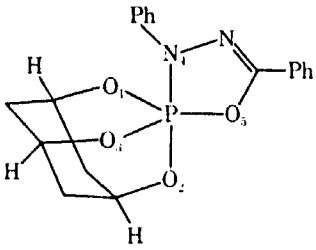

ACKNOWLEDGEMENT

This investigation was supported by grants from the National Science Foundation (MPS 74-11496) and from the National Institutes of Health (GM 21466), which are gratefully acknowledged. We are also grateful to the University of Massachusetts Computer Center for generous allocation of computer time.

REFERENCES AND NOTES

1. Pentacoordinated Molecules. 21. Previous paper in this series: R. R. Holmes, *J. Am. Chem. Soc.*, **97,** 5379 (1975).
2. Extensive reviews of the NMR data are found in the following sources: (a) R. Lukenbach, "Dynamic Stereochemistry of Pentacoordinated Phosphorus and Related Elements," George Thieme Verlag, Stuttgart, 1973; (b) D. Hellwinkel, "Organo Phosphorus Compounds," Vol. 3, G. M. Kosolapoff and L. Maier, Ed., Wiley-Interscience, New York, N.Y., 1972, p 185.
3. R. S. Berry, *J. Chem. Phys.*, **32,** 933 (1960).
4. D. Z. Denney, D. W. White and D. B. Denney, *J. Am. Chem. Soc.*, **93,** 2066 (1971).
5. (a) P. Gillespie, P. Hoffmann, H. Klusacek, D. Marquarding, S. Pfohl, F. Ramirez, E. A. Tsolis and I. Ugi, *Angew. Chem., Int. Ed. Engl.*, **10,** 687 (1971); (b) F. Ramirez and I. Ugi, *Adv. Phys. Org. Chem.*, **9,** 256 (1971); (c) I. Ugi, F. Ramirez, D. Marquarding, H. Klusacek and P. Gillespie, *Acc. Chem. Res.*, **4,** 288 (1971); (d) F. Ramirez and I. Ugi, *Bull. Soc. Chim. Fr.*, 453 (1974).
6. (a) H. Wunderlich, D. Mootz, R. Schmutzler and M. Wieber, *Z. Naturforsch. B*, **29,** 32 (1974); (b) H. Wunderlich, *Acta Crystallogr., Sect. B*, **30,** 939(1974); (c) H. Wunderlich and D. Mootz, *ibid.*, **30,** 935 (1974).
7. R. R. Holmes, *J. Am. Chem. Soc.*, **96,** 4143 (1974).
8. E. L. Muetterties and L. J. Guggenberger, *J. Am. Chem. Soc.*, **96,** 1748 (1974).
9. (a) R. K. Brown and R. R. Holmes, *J. Am. Chem. Soc.*, **99,** 3326 (1977); (b) P. F. Meunier, J. A. Deiters and R. R. Holmes, *Inorg. Chem.*, **15,** 2572 (1976); (c) P. F. Meunier, J. R. Devillers and R. R. Holmes, work submitted for publication.
10. J. R. Devillers and R. R. Holmes, *J. Am. Chem. Soc.*, **99,** 3332 (1977).
11. J. A. Deiters, J. C. Gallucci, T. E. Clark and R. R. Holmes, work submitted for publication.
12. R. Sarma, F. Ramirez and J. F. Maracek, *J. Org. Chem.*, **41,** 473 (1976).
13. D. D. Swank, C. N. Caughlan, F. Ramirez and J. F. Pilot, *J. Am. Chem. Soc.*, **93,** 5236 (1971).
14. R. Sarma, F. Ramirez, B. McKeever, J. F. Maracek and S. Lee, *J. Am. Chem. Soc.*, **98,** 581 (1976).
15. (a) W. C. Hamilton, S. J. LaPlaca and F. Ramirez, *J. Am. Chem. Soc.*, **87,** 127 (1965); (b) R. D. Spratley, W. C. Hamilton and J. Ladell, *ibid.*, **89,** 2272 (1967).
16. (a) W. C. Hamilton, J. S. Ricci, Jr., F. Ramirez, L. Kramer and P. Stern, *J. Am. Chem. Soc.*, **95,** 6335 (1973); (b) H. L. Carrell, H. M. Berman, J. S. Ricci, Jr., W. C. Hamilton, F. Ramirez, J. F. Marecek, L. Kramer and I. Ugi, *ibid.*, **97,** 38 (1975).
17. D. Hellwinkel, W. Krapp, D. Schomburg and W. S. Sheldrick, *Z. Naturforsch. B*, **31,** 948 (1976).
18. (a) W. S. Sheldrick, A. Schmidpeter and J. H. Weinmaier, *Angew. Chem.*, **87,** 519 (1975); (b) W. S. Sheldrick, *Acta Crystallogr., Sect. B*, **32,** 925 (1976).
19. W. S. Sheldrick, personal communication; A. Schmidpeter, D. Schomburg, W. S. Sheldrick and J. H. Weinmaier, *Angew. Chem.*, **88,** 851 (1976).
20. W. S. Sheldrick, personal communication.
21. M. Eisenhut, R. Schmutzler and W. S. Sheldrick, *J. Chem. Soc., Chem. Commun.*, **144** (1973), and personal communication.
22. This column is simply obtained by noting which observed angles fall outside the range of the values of the respective angles traversed between the idealized TP and SP (RP) structures (Figure 3),

measuring the number of degrees that each fall outside the range, taking their sum, and multiplying by two.
23. Nine dihedral angles are given based on the idealized TP geometry in Figure 3(a). Additional dihedral angles arise for actual structures but are not common to the idealized structures being used for comparison.
24. (a) A. Rauk, L. C. Allen and K. Mislow, *J. Am. Chem. Soc.*, **94,** 3035 (1972); (b) R. Hoffmann, J. M. Howell and E. L. Muetterties, *ibid.*, **94,** 3047 (1972); (c) L.S. Bartell and V. Plato, *ibid.*, **95,** 3097 (1973); (d) A. Strich and A. Veillard, *ibid.*, **95,** 5574 (1973).
25. (a) R. R. Holmes, *Acc. Chem. Res.*, **5,** 296 (1972); (b) R. R. Holmes, L. S. Couch and C. J. Hora, Jr., *J. Chem. Soc., Chem. Commun.*, 197 (1974).
26. L. S. Bernstein, J. J. Kim, K. S. Pitzer, S. Abramowitz and I. Levin, 30th Symposium on Molecular Structure and Spectroscopy. The Ohio State University, Columbus, Ohio, June 1975, Abstract No. TA6; L. S. Bernstein, S. Abramowitz and I. W. Levin, *J. Chem. Phys.*, **64,** 3328 (1976); L. S. Bernstein, J. J. Kim, K. S. Pitzer, S. Abramowitz and I. W. Levin, *ibid.*, **62,** 3671 (1975).
27. (a) L. S. Bartell, *Inorg. Chem.*, **9,** 1594 (1970); (b) K. W. Hansen and L. S. Bartell, *ibid.*, **4,** 1775 (1965); (c) L. S. Bartell and K. W. Hansen, *ibid.*, **4,** 1777 (1965); (d) F. B. Clippard, Jr., and L. S. Bartell, *ibid.*, **9,** 805 (1970); (e) W. J. Adams and L. S. Bartell, *J. Mol. Struct.*, **8,** 23 (1971); (f) H. Yow and L. S. Bartell, *ibid.*, **15,** 209 (1973).
28. (a) J. E. Griffiths, R. P. Carter, Jr. and R. R. Holmes, *J. Chem. Phys.*, **41,** 863 (1964); (b) I. W. Levin, *ibid.*, **50,** 1031 (1969); (c) F. A. Miller and R. J. Capwell, *Spectrochim. Acta, Part A*, **27,** 125 (1971); (d) I. W. Levin, *J. Mol. Spectrosc.*, **33,** 61 (1970).
29. As previously cited[7,25a] electron-pair repulsion considerations, with reference to the idealized SP in Figure 3(b), suggest a correspondence in bond properties between the basal bonds of the SP and axial bonds of the TP. Thus, the more electronegative ligands would prefer the basal positions of the SP and small-membered rings would locate in a cis-basal rather than a basal-axial pair. The latter correspondence for the SP follows from the element and strain rules for the TP.[30]
30. (a) F. H. Westheimer, *Acc. Chem. Res.*, **1,** 70 (1968); (b) E. L. Muetterties, W. Mahler and R. Schmutzler, *Inorg. Chem.*, **2,** 613 (1963); (c) E. L. Muetterties, W. Mahler, K. J. Packer and R. Schmutzler, *ibid.*, **3,** 1298 (1964).
31. J. A. Howard, D. R. Russell and S. Trippett, *J. Chem. Soc., Chem. Commun.*, 856 (1973).
32. A. Schmidpeter, J. Luber, D. Schomburg and W. S. Sheldrick, *Chem. Ber.*, in press.
33. M.-Ul-Haque, C. N. Caughlan, F. Ramirez, J. F. Pilot and C. P. Smith, *J. Am. Chem. Soc.*, **93,** 5229 (1971).
34. K. Mislow, *Acc. Chem. Res.*, **3,** 321 (1970).
35. (a) D. Gorenstein and F. H. Westheimer, *J. Am. Chem. Soc.*, **92,** 634 (1970); (b) D. Gorenstein, *ibid.*, **92,** 664 (1970).
36. F. Ramirez, *Acc. Chem. Res.*, **1,** 168 (1968).